Biochimica et Biophysica Acta 819 (1985) 153–160
Elsevier

BBA 72730

The interaction of calcium with gangliosides in bilayer membranes

Robert McDaniel and Stuart McLaughlin

Department of Physiology and Biophysics, Health Sciences Center, State University of New York at Stony Brook, Stony Brook, NY 11794 (U.S.A.)

(Received June 3rd, 1985)

Key words: Phospholipid bilayer; Ganglioside; Ca^{2+}; Electrostatic potential; Electrophoretic mobility

We studied the binding of calcium to bilayer membranes formed from mixtures of phosphatidylcholine and mono-, di-, or trisialoganglioside by measuring its effect on the electrophoretic mobility of multilamellar vesicles and the conductance of planar bilayers. In 0.001 M monovalent salt solutions the surface potential of the membranes is large and micromolar concentrations of calcium have a significant effect on the mobility and conductance. In 0.1 M monovalent salt solutions the surface potential is small and millimolar concentrations of calcium are required to affect these parameters. The strong apparent binding of calcium we observed at low ionic strength could be due to the nonspecific accumulation of calcium in the electrical diffuse double layer. To distinguish between this nonspecific effect and binding of calcium to the membrane, we substituted dimethonium for calcium. Dimethonium is a divalent cation that screens negative charges but does not bind to lipids. We also examined the effect of replacing phosphatidylcholine by monoolein: calcium binds to phosphatidylcholine but not to monoolein. We describe our electrophoretic mobility results by combining the Poisson-Boltzmann and Navier-Stokes equations with the Langmuir adsorption isotherm. We conclude that calcium binds weakly to gangliosides with an intrinsic association constant of $< 100\ M^{-1}$, which is similar to the association constant of calcium with phospholipids.

Introduction

The interaction of calcium (Ca) with gangliosides has been studied by calorimetry [1–3], bilayer adhesion [4], monolayer [5–6], solubility [7], pH titration [8], electron paramagnetic resonance [9–10], and calcium-selective electrode [11–14] measurements.

Behr and Lehn [11] and Probst et al. [13] studied the binding of Ca to G_{M1}, G_{D1a}, or G_{T1} micelles in solutions of low (millimolar) ionic strength. Behr and Lehn calculated an apparent Ca-G_{D1a} association constant of $6 \cdot 10^4\ M^{-1}$ and Probst et al. calculated an apparent Ca-G_{M1} association constant of $2 \cdot 10^6\ M^{-1}$. The apparent association constants decrease when the ionic strength increases: in decimolar monovalent salt solutions, these constants are less than $100\ M^{-1}$ [14]. We suspected that the large apparent association constants measured in solutions of low ionic strength are due to the accumulation of Ca in the aqueous phase adjacent to the ganglioside micelles because of the large negative electrostatic potential, ψ, that exists in the aqueous phase adjacent to the binding sites on the gangliosides. According to the Boltz-

Abbreviations: FCCP, carbonyl cyanide *p*-trifluoromethoxyphenylhydrazone; G_{D1a}, *N*-acetylneuraminylgalactosyl-*N*-acetylgalactosaminyl(*N*-acetylneuraminyl)galactosylglucosylceramide; G_{M1}, galactosyl-*N*-acetylgalactosaminyl(*N*-acetylneuraminyl)galactosylglucosylceramide; G_{T1}, *N*-acetylneuraminylgalactosyl-*N*-acetylgalactosaminyl(*N*-acetylneuraminyl-*N*-acetylneuraminyl)galactosylglucosylceramide; Mops, 4-morpholinepropane sulfonate; PC, phosphatidylcholine.

mann relation the apparent association constant (K_{app}) is related to the intrinsic association constant (K_{int}) by

$$K_{app} = K_{int} \exp(-2F\psi/RT) \quad (1)$$

where F is the Faraday, R is the gas constant and T is the absolute temperature. $K_{app} = K_{int}$ when $\psi = 0$.

We made two types of measurements to calculate K_{int}. First, we formed planar bilayers from mixtures of PC or glycerol monooleate with gangliosides G_{M1}, G_{D1a}, or G_{T1} and measured the effect of Ca on the conductance due to nonactin-K to estimate the change in electrostatic potential within the bilayers. Second, we formed multilamellar vesicles from these mixtures of lipids and measured the effect of Ca on their electrophoretic mobility.

We used Langmuir adsorption isotherms (mass action) to describe the relationship between the number of calcium ions bound to the gangliosides or PC molecules and concentration of Ca in the aqueous phase adjacent to the binding sites. We related this concentration to the concentration of Ca in the bulk aqueous phase by means of the Boltzmann relation (see Eqn. 1). To calculate the profile of electrostatic potential adjacent to the gangliosides, we used the linearized Poisson-Boltzmann equation and assumed the charges are 1 nm from the bilayer surface. To describe the electrophoretic mobility results, we combined this potential profile with a form of the Navier-Stokes equation that includes a hydrodynamic drag term due to the ganglioside head groups.

We conclude that the intrinsic association constant of Ca with gangliosides is small (0–100 M^{-1}), comparable to the association constants of Ca with sialic acid (2.5–121 M^{-1}, [15,16]) and most charged phospholipids (10 M^{-1}, [17]).

Materials and Methods

Calcium chloride dihydrate (grade I) was obtained from Sigma (St. Louis, MO). Dimethonium bromide was synthesized as previously described [18]. Water was deionized (Super-Q, Millipore Corp., Bedford, MA) then bidistilled in quartz still. Methanol (HPLC grade, Aldrich Chem. Co., Chicago, IL) was redistilled before use. Sodium and potassium chloride were heated to 550°C to remove organic impurities. For the electrophoresis experiments we used 0.001 M or 0.1 M NaCl solutions and for the conductance experiments we used 0.001 M or 0.1 M KCl solutions. Monovalent salt solutions were buffered with 0.0001–0.005 M Mops to pH 7.4 at 25°C. These solutions were initially free of Ca because 10 μM EDTA had no effect on the electrophoretic mobility or nonactin-K conductance. Gangliosides G_{M1}, G_{D1a}, and G_{T1} were obtained from Supelco (Bellafonte, PA) and ran as single major spots on thin-layer chromatograms (Silica Gel G, developed in chloroform/methanol/0.02% aqueous $CaCl_2$, 60 : 30 : 10, v/v). We used diphytanoylphosphatidylcholine for the planar bilayer experiments and egg phosphatidylcholine for the microelectrophoresis experiments: both were obtained from Avanti Biochemicals (Birmingham, AL). Glycerol monooleate was obtained from Nu-Chek Prep (Elysian, MN). Either PC or glycerol monooleate was mixed with ganglioside in spectrograde chloroform or methanol/H_2O (33 : 1, v/v) and the solvent was removed by rotary evaporation. We used either PC/ganglioside (2.5 : 1, w/w) or glycerol monooleate/ganglioside (2.3 : 1, w/w) mixtures to form the membranes. We calculated the charge density of these membranes by assuming that one charge is on each sialic acid residue and that each acyl chain occupies an area of 0.35 nm^2. Analysis of the gangliosides by the supplier gave 0.95, 1.88, and 2.55 moles of sialic acid per mole of G_{M1}, G_{D1a}, and G_{T1}, respectively. Thus, there were 0.08, 0.15, and 0.20 negative charges per lipid acyl chain for membranes containing gangliosides G_{M1}, G_{D1a}, and G_{T1}, respectively.

Electrophoretic mobilities (μ) were measured in a Mark I microelectrophoresis cell (Bottisham, Cambridge, U.K.) and the mobilities were converted to apparent zeta potentials [19] by Eqn. 2, the Helmholtz-Smoluchowski equation

$$\zeta = \mu\eta/\epsilon_0\epsilon_r \quad (2)$$

where ζ is the apparent zeta potential, ϵ_0 is the permittivity of free space, ϵ_r is the dielectric constant, and η is the viscosity [20].

The electrostatic potential within planar bilayers was estimated from steady-state conductance measurements using nonactin-K [21]. Non-

actin was a gift of B. Stearns (Squibb, New Brunswick, NJ). Addition of Ca caused the nonactin-K conductance of planar bilayers to decrease. To verify that this decrease was due to a positive shift in electrostatic potential within the bilayer, we measured the conductance due to the anionic probes FCCP and tetraphenylborate. For both PC-ganglioside and glycerol monooleate-ganglioside bilayers, addition of Ca caused the conductance of these anionic probes to increase. The increase in conductance due to the anionic probes upon adding Ca to a PC-ganglioside membrane is less, by a factor of about 2, than the corresponding decrease in nonactin-K conductance. This asymmetry may arise from a non-electrostatic effect, such as a decrease in the fluidity or dielectric constant. We calculated the change in electrostatic potential within bilayers due to Ca from the nonactin-K measurements. Thus, we may be overestimating the effect of Ca, which strengthens our basic conclusion that it interacts weakly with gangliosides.

Results

Fig. 1 illustrates the effect of Ca on the apparent zeta potential of PC-G_{M1} vesicles and the electrostatic potential within PC-G_{M1} planar bilayers. When we formed the vesicles and planar bilayers in monovalent salt solutions of low (0.001 M) ionic strength, addition of micromolar concentrations of Ca changed both potentials (open symbols). In salt solutions of high (0.1 M) ionic strength millimolar concentrations of Ca are required to change the potentials (filled symbols). Fig. 1 illustrates that the apparent association constant for the binding of Ca to PC-ganglioside membranes decreases as the ionic strength increases. Others [11–14,22] obtained similar results for the binding of Ca to ganglioside micelles. These results are expected theoretically because the electrostatic potential in the aqueous phase adjacent to the gangliosides depends on the salt concentration. As the ionic strength increases the magnitude of this potential decreases and less Ca accumulates near the negative charges on gangliosides. This decreases the apparent Ca-ganglioside association constant (see Eqn. 1).

To quantitatively describe the effect of Ca on

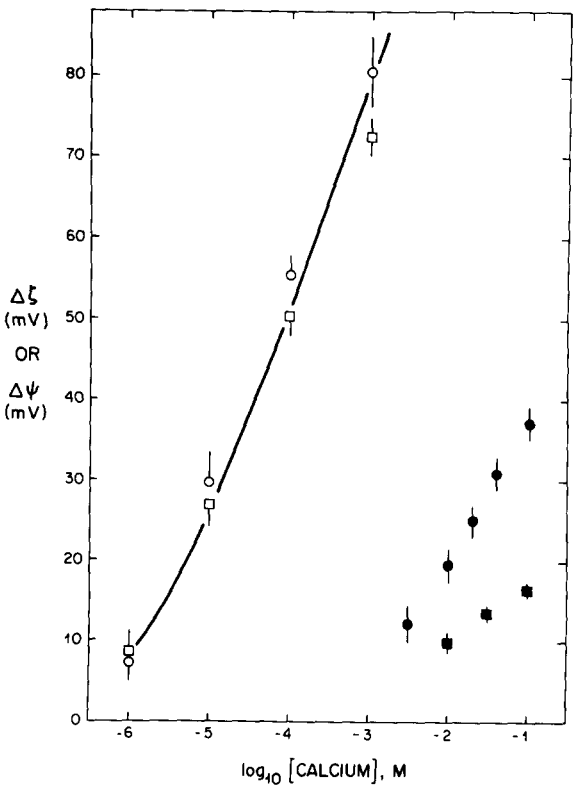

Fig. 1. The effect of ionic strength on the interaction of calcium with 2.5:1 (w/w) PC-G_{M1} membranes. The open symbols represent measurements in 0.001 M monovalent salt solutions (zeta = -98.5 ± 3.5 mV at [Ca] = 0). The filled symbols represent measurements in 0.1 M monovalent salt solutions (zeta = -16 mV at [Ca] = 0). Squares represent the shifts in apparent zeta potentials of multilamellar vesicles, as determined from electrophoretic mobility measurements. Circles represent the shifts in electrostatic potentials within planar bilayers, as determined from nonactin-K conductance measurements. The curve is the prediction of the Grahame equation [20] assuming that Ca does not bind to the membrane (surface charge density = -0.24 charges/nm^2). In all the figures, the vertical lines represent the standard deviations of 20 zeta potential measurements and five planar bilayer measurements.

the electrostatic potential, we applied diffuse double layer theory. We first note that in 0.001 M monovalent salt solutions the Debye length (10 nm) is larger than the ganglioside head group (approx. 2 nm). To calculate the curve of Fig. 1, we assumed that the fixed charges and hydrodynamic shear plane are at the bilayer surface and that the ganglioside head groups exert no hydrodynamic drag. Under these conditions, the surface potential equals the zeta potential and the

Grahame equation [20,23] relates the surface potential to the density of surface charges. If we assume that no Ca binds to the membrane, these surface charges exist only on sialic acid groups. Since the curve in Fig. 1 describes the data, it is not necessary to postulate a strong binding of Ca to ganglioside to explain the high apparent association constant when the ionic strength is low.

The situation is more complicated when the ionic strength is 0.1 M because the Debye length (1 nm) is comparable to the size of the ganglioside head group (approx. 2 nm). If the charges are located a significant distance from the surface, the magnitude of the surface potential will decrease and the magnitude of the electrophoretic mobility will increase [19]. We must also account for the hydrodynamic drag exerted by the extended ganglioside head groups, which will decrease the magnitude of the electrophoretic mobility. Calcium ions could change the electrophoretic mobility and the electrostatic potential adjacent to the PC-ganglioside bilayer by: (i) screening the fixed negative charges on the gangliosides, (ii) binding to PC, or (iii) binding to ganglioside. We tried to separate these effects with the following experiments.

We formed six types of bilayers by mixing either the zwitterionic lipid PC or the neutral lipid glycerol monooleate with the gangliosides G_{M1}, G_{D1a}, or G_{T1}. These gangliosides have 1, 2, and 3 negative charges, respectively. To investigate the screening of the negative charges by divalent cations, we replaced calcium with dimethonium. This divalent cation changes the potential of charged bilayers by screening fixed negative charges, but it does not bind to lipid membranes [18]. The results are shown in Fig. 2. Addition of dimethonium shifts the apparent zeta potential of PC-ganglioside or glycerol monooleate-ganglioside vesicles and the potential within planar bilayers to more positive values. These shifts in potential are small (less than 15 mV). They illustrate the magnitude of the screening effect exerted by divalent cations on bilayer membranes containing gangliosides. Thus, we can compare the effects of dimethonium and Ca on these membranes to estimate the screening effect of Ca.

The effects of Ca on PC-ganglioside membranes are shown in Fig. 3. 0.1 M dimethonium shifts the surface potential of PC-G_{M1} bilayers by 6 mV

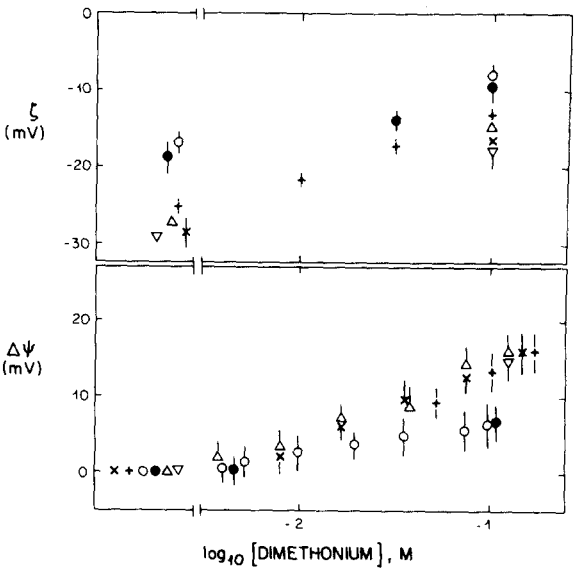

Fig. 2. The effect of dimethonium bromide on the apparent zeta potentials of multilamellar vesicles (upper panel) and potentials within planar bilayers (lower panel). Bilayers were formed in 0.1 M monovalent salt solutions from 2.5:1 (w/w) mixtures of PC with G_{M1} (○), G_{D1a} (+) or G_{T1} (△), or from 2.3:1 (w/w) mixtures of glycerol monooleate with G_{M1} (●), G_{D1a} (×) or G_{T1} (▽).

(Fig. 2) but 0.1 M Ca shifts the surface potential by 38 mV (Fig. 3A). Similar results were obtained with PC-G_{D1a} and PC-G_{T1} bilayers: the change in surface potential produced by Ca (Figs. 3B, 3C) is about three times the change produced by dimethonium (Fig. 2). These results indicate that a nonspecific screening effect can account for only part of the interaction of Ca with PC-ganglioside membranes *.

We suspected that some of this interaction could be due to binding of Ca to the PC head group. PC binds calcium ions [17,25] and the thermal properties of PC-ganglioside bilayers may be dominated by the binding of Ca to PC [3]. Also, PC-ganglioside vesicles bind more Ca than do ganglioside micelles [14].

To eliminate the Ca-PC interaction, we formed glycerol monooleate-ganglioside membranes [24]

* Although dimethonium exerts only a slightly smaller effect on the apparent zeta potential than does Ca, this result is predicted by the quantitative analysis we present in the Appendix.

because glycerol monooleate does not bind Ca [17]. In the absence of Ca, glycerol monooleate-ganglioside vesicles have about the same electrophoretic mobility as PC-ganglioside vesicles (see Fig. 2 and points to the left in the upper panels of Figs. 3 and 4). Thus, glycerol monooleate-ganglioside membranes are useful for comparison with PC-ganglioside membranes. The effect of Ca on glycerol monooleate-ganglioside bilayers is shown in Fig. 4. Ca causes positive shifts in the surface and apparent zeta potentials. The magnitudes of these shifts are similar to those caused by dimethonium (Fig. 2), suggesting that screening of charges on ganglioside can account for most of the effect of Ca on these membranes.

Ca shifts the surface potential of glycerol monooleate-ganglioside bilayers (Fig. 4) only half as much as PC-ganglioside bilayers (Fig. 3) because Ca binds to the phosphate group of PC, which is located at the surface of the bilayer. However, this large difference in the effect of Ca on the surface potential leads to a small difference in the effect of Ca on the apparent zeta potential (compare Figs. 3 and 4). This result is expected because the ganglioside head groups exert a hydrodynamic drag that diminishes the effect of surface charge on the

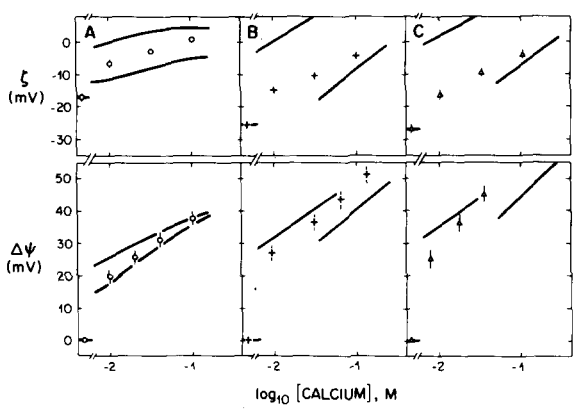

Fig. 3. The effect of calcium on apparent zeta potentials of multilamellar PC-ganglioside vesicles (upper panels) and potentials within PC-ganglioside planar bilayers (lower panels). Bilayers were formed from 2.5:1 (w/w) mixtures of PC and ganglioside G_{M1} (A), G_{D1a} (B), or G_{T1} (C). The upper curve in each panel represents the theoretical prediction if the Ca-ganglioside intrinsic association constant is 100 M^{-1}, and the lower curve represents the theoretical prediction if it is 0 M^{-1}. We assumed that the Ca-PC intrinsic association constant is 3 M^{-1}. The other assumptions are discussed in the appendix.

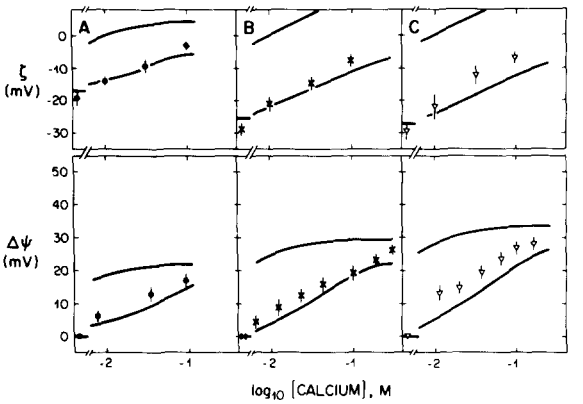

Fig. 4. The effect of calcium on zeta potentials of multilamellar glycerol monooleate-ganglioside vesicles (upper panels) and potentials within glycerol monooleate-ganglioside planar bilayers (lower panels). Bilayers were formed from 2.3:1 (w/w) mixtures of glycerol monooleate and ganglioside G_{M1} (A), G_{D1a} (B), or G_{T1} (C). As in Fig. 3, the upper curve in each panel represents the theoretical prediction if the Ca-ganglioside intrinsic association constant is 100 M^{-1}, and the lower curve represents the theoretical prediction if it is 0 M^{-1}. Ca does not bind to glycerol monooleate.

electrophoretic mobility [19]. Furthermore, the negative charges on gangliosides are located about a Debye length away from the surface of the bilayer and have a larger influence on the electrophoretic mobility than do calcium ions bound to the surface of the bilayer [19].

We calculated theoretically the effect of Ca on the surface potential and on the electrophoretic mobility. We made the following assumptions: (1) Ca binds to PC with an intrinsic association constant of 3 M^{-1} [17,25]; (2) the fixed charges on gangliosides are 1 nm from the bilayer surface [19,26,27]; (3) the gangioside head groups extend about 2 nm from the bilayer surface and each mnosaccharide exerts a hydrodynamic drag equivalent to an independent sphere of Stokes radius 0.35 nm [19,27]. We calculated the effect of Ca on the surface potential from the Poisson-Boltzmann and Langmuir adsorption equations and we combined these equations with the Navier-Stokes equation to calculate the effect of Ca on the electrophoretic mobility. The theoretical results are shown as the curves in Figs. 3 and 4, where the data are bracketed by assuming that the Ca-ganglioside intrinsic association constant is 0 or 100 M^{-1} (see Appendix).

Discussion

We accounted for the effect of electrostatic potentials on the interaction of Ca with gangliosides by applying the Poisson-Boltzmann, Navier-Stokes, and Langmuir adsorption equations to our data. We concluded that the intrinsic association constant of Ca with the gangliosides G_{M1}, G_{D1a}, and G_{T1} is below 100 M^{-1}. Previously, Behr and Lehn [11], Muhleisen et al. [12], and Probst et al. [13] calculated the Ca-ganglioside association constant by using Scatchard plots. In making this calculation, they implicitly assumed that the concentration of Ca in the aqueous phase adjacent to the gangliosides is equal to its concentration in the bulk aqueous phase. This assumption is incorrect because the negative electrostatic potential adjacent to the ganglioside micelle enhances the local concentration of Ca. For example, if the surface potential of ganglioside micelles in millimolar salt solutions is −120 mV, the apparent Ca-ganglioside association constant obtained from a Scatchard analysis by Probst et al. [13] (about 10^6 M^{-1}) will differ from the intrinsic Ca-ganglioside association constant by four orders of magnitude (Eqn. 1). This would reconcile our results with the findings of Probst et al. [13]. Furthermore, our suggestion that the intrinsic Ca-ganglioside association constant is below 100 M^{-1} is consistent with the measured value of the Ca-sialic acid association constant [15,16].

Previous studies [11–14] demonstrated that the interaction of Ca with gangliosides decreases as the ionic strength increases. We agree (Fig. 1). Our experimental results and theoretical analysis suggest that this effect is due to monovalent ions in the aqueous diffuse double layer 'screening' the charges on gangliosides and reducing the magnitude of the electrostatic potential adjacent to the membrane [23].

It has been suggested [5–6,12,22] that gangliosides are specific receptors for calcium in biological membranes. However, the intrinsic association constant for binding of Ca to gangliosides is small (0–100 M^{-1}), comparable to that of most phospholipids [Table 3 in Ref. 25]. Thus, we consider it unlikely that biological membranes use gangliosides as receptors for calcium.

Appendix

We make the conventional assumptions inherent in the Gouy-Chapman-Stern theory: the ions are point charges, the dielectric constant of the aqueous phase is uniform, and image charge effects are negligible. We also assume that the charges on gangliosides are uniformly smeared in a plane at $x = 0$, which is 1 nm from the bilayer surface located at $x = -b$ [19,26,27]. The surface concentration (units of nm^{-2}) of sialic acid at $x = 0$ is denoted {S}. The charge density in this plane, $\sigma_o = -e\{S\}$ at [Ca] = 0, where e is the magnitude of the electronic charge. The surface concentration of PC at $x = -b$ is denoted {PC} and the charge density of the bilayer surface, σ_i, is zero before the addition of calcium. Ca in aqueous solution, at bulk concentration [Ca], may bind to the outer plane at $x = 0$ with an intrinsic association constant of K_o or to the inner plane at $x = -b$ with an intrinsic association constant of K_i. We assume that Ca binds by Langmuir adsorption (mass action). K_o and K_i are equilibrium constants for the binding reactions

$$\text{Ca} + \text{S} \rightleftarrows \text{Ca-S} \qquad K_o = \frac{\{\text{Ca-S}\}}{[\text{Ca}]_{x=0}\{\text{S}\}_f} \tag{3}$$

$$\text{Ca} + \text{PC} \rightleftarrows \text{Ca-PC} \qquad K_i = \frac{\{\text{Ca-PC}\}}{[\text{Ca}]_{x=-b}\{\text{PC}\}_f} \tag{4}$$

where f denotes free concentrations and

$$\{\text{S}\}_f = \{\text{S}\} - \{\text{Ca-S}\};\ \{\text{PC}\}_f = \{\text{PC}\} - \{\text{Ca-PC}\}$$

The divalent positive complex, Ca-PC, is the only charged species at $x = -b$. At $x = 0$, there are two charged species: the monovalent negative sialic acid on ganglioside, S, and the monovalent positive complex, Ca-S. The charge densities of the planes at $x = 0$, σ_i, and $x = -b$, σ_o, are

$$\sigma_i = 2e\{\text{Ca-PC}\} \tag{5}$$

$$\sigma_o = -e\{\text{S}\} + e\{\text{Ca-S}\} \tag{6}$$

The aqueous concentrations of calcium at $x = 0$ and $x = -b$ are given by the Boltzmann relation

$$[\text{Ca}]_{x=0} = [\text{Ca}]\exp(-2F\psi(0)/RT) \tag{7}$$

$$[\mathrm{Ca}]_{x=-b} = [\mathrm{Ca}]\exp(-2\mathrm{F}\psi(-b)/RT) \quad (8)$$

where $\psi(x)$ is the electrostatic potential at position x. Combining Eqns. 3–8, we obtain two relations between potential and charge density at $x = -b$ and at $x = 0$.

$$\sigma_i = \frac{2e\{\mathrm{PC}\}K_i[\mathrm{Ca}]\exp(-2F\psi(-b)/RT)}{1+K_i[\mathrm{Ca}]\exp(-2F\psi(-b)/RT)} \quad (9)$$

$$\sigma_o = \frac{-e\{\mathrm{S}\}+e\{\mathrm{S}\}K_o[\mathrm{Ca}]\exp(-2F\psi(0)/RT)}{1+K_o[\mathrm{Ca}]\exp(-2F\psi(0)/RT)} \quad (10)$$

Two relations between potential and charge density at $x = 0$ and $x = -b$ are obtained from Gauss' law:

$$\text{at } x=0 \quad \left.\frac{d\psi(x)}{dx}\right|_{x=0+} - \left.\frac{d\psi(x)}{dx}\right|_{x=0-} = (-1/\epsilon_0\epsilon_r)\sigma_o \quad (11)$$

$$\text{at } x=-b \quad \frac{d\psi(x)}{dx} = (-1/\epsilon_0\epsilon_r)\sigma_i \quad (12)$$

We use the linearized Poisson -Boltzmann equation to describe the dependence of potential on distance. This second order differential equation relates the space charge density of mobile ions to the potential at x when the mangitude of the potential is less than 13 mV. When the potentials were outside this range, we used the nonlinear theory of Sharp et al. [28] if K_i and K_o were zero. $1/\kappa$ is the Debye length (nm). The general solution of the linearized Poisson-Boltmann equation for the case of two fixed charge planes [29] is

$$-b < x < 0 \quad \psi(x) = A\exp(-\kappa x) + B\exp(\kappa x) \quad (13)$$

$$x > 0 \quad \psi(x) = C\exp(-\kappa x) \quad (14)$$

where A, B, and C are constants of integration, whose value is determined by application of boundary conditions at $x = -b$ and $x = 0$ (Eqns. 11 and 12). Also, the potential is continuous at $x = 0$ (Eqns. 13 and 14). From the third boundary condition, we obtain A, B, and C as a function of $\psi(-b)$ and $\psi(0)$

$$A = [\psi(0)\exp(-\kappa b) - \psi(-b)]/[\exp(-\kappa b) - \exp(\kappa b)] \quad (15)$$

$$B = \psi(0) - A \quad (16)$$

$$C = A + B = \psi(0) \quad (17)$$

By combining Eqns. 9–17 and eliminating σ_i and σ_o, we obtain two equations in two unknowns which provide the values of $\psi(-b)$ and $\psi(0)$ when solved simultaneously by an iterative two-dimensional Newton-Raphson procedure. These two equations are:

$$\begin{aligned}\psi(0) = {} & [(-e\{\mathrm{S}\}/2\kappa\epsilon_0\epsilon_r)(1+\exp(-2\kappa b)) \\ & \times (1-K_o[\mathrm{Ca}]\exp(-2F\psi(0)/RT))] \\ & \times [1+K_o[\mathrm{Ca}]\exp(-2F\psi(0)/RT)]^{-1} \\ & + [(2e\{\mathrm{PC}\}/\kappa\epsilon_0\epsilon_r)\exp(-\kappa b) \\ & \times K_i[\mathrm{Ca}]\exp(-2F\psi(-b)/RT)] \\ & \times [1+K_i[\mathrm{Ca}]\exp(-2F\psi(-b)/RT)]^{-1}\end{aligned} \quad (18)$$

$$\begin{aligned}\psi(-b) = {} & [(-e\{\mathrm{S}\}/\kappa\epsilon_0\epsilon_r)\exp(-\kappa b) \\ & \times (1-K_o[\mathrm{Ca}]\exp(-2F\psi(0)/RT))] \\ & \times [1+K_o[\mathrm{Ca}]\exp(-2F\psi(0)/RT)]^{-1} \\ & + [(2e\{\mathrm{PC}\}/\kappa\epsilon_0\epsilon_r) \\ & \times K_i[\mathrm{Ca}]\exp(-2F\psi(-b)/RT)] \\ & \times [1+K_i[\mathrm{Ca}]\exp(-2F\psi(-b)/RT)]^{-1}\end{aligned} \quad (19)$$

We substitute the values of $\psi(0)$ and $\psi(-b)$ obtained from Eqns. 18 and 19 into Eqns. 15–17, which gives A, B, and C. By substitution of A, B, and C into Eqns. 13 and 14 we obtain the potential at any distance x.

We used the Navier-Stokes equation to calculate the electrophoretic mobility, μ, from a knowledge of the potential distribution. We used a form of the Navier-Stokes equation that includes a force term due to the hydrodynamic drag exerted by ganglioside head groups [19,27–29]. We assumed that each monosaccharide in these head groups is an independent sphere of Stokes radius 0.35 nm. Following Levine et al. [29] the general solution of the Navier-Stokes equation for electro-osmotic flow adjacent to a fixed membrane is

$$x > b' \quad u(x) = (1/\eta)\epsilon_0\epsilon_r E\psi(x) + U \quad (20)$$

$$-b < x < b' \quad u(x) = P\exp(-gx) + Q\exp(gx) + (1/\eta)g'\epsilon_0\epsilon_r E\psi(x) \quad (21)$$

$$\text{where} \quad g' = \kappa^2/(\kappa^2 - g^2) \quad \text{for } (g/\kappa) \gg 1 \quad (22)$$

$$\text{and} \quad g = (Nf/\eta)^{0.5} \quad (23)$$

where E is the applied electric field and N is the number density of ganglioside head group monosaccharides. Each monosaccharide exerts a hydrodynamic drag force f, and the monosaccharides are uniformly distributed from $x = -b$ to $x = b'$. We assume that the distance from $x = -b$ to $x = b'$ is 2.0, 2.1 and 2.3 nm for gangliosides G_{M1}, G_{D1a}, and G_{T1}, respectively. These distances were determined from a fit of the apparent zeta potential data in the absence of Ca (Fig. 3). P, Q, and U are constants of integration whose values are determined by application of the boundary conditions:

$u(-b) = 0$ i.e. the hydrodynamic plane of shear is at the bilayer surface (24)

$u(x)$ is continuous at $x = b'$ (25)

$\frac{du(x)}{dx}$ is continuous at $x = b'$ (26)

Eqn. 22 diverges when κ approaches g. In this case, the general solution of the Navier-Stokes equation becomes:

$$-b < x < 0 \quad u(x) = P\exp(-\kappa x) + Q\exp(\kappa x) + (E\kappa x/2\eta)\epsilon_0\epsilon_r(-A\exp(-\kappa x) + B\exp(\kappa x)) \quad (27)$$

$$0 < x < b' \quad u(x) = P\exp(-\kappa x) + Q\exp(\kappa x) + (-E\kappa x/2\eta) \times \epsilon_0\epsilon_r(A + B)\exp(-\kappa x) \quad (28)$$

By eliminating P and Q in Eqns. 21, 27, and 28 we solve for U as a function of the potential at $x = 0$. U is the electro-osmotic fluid velocity several Debye lengths from the surface of the membrane, so $-U/E$ is equal to the electrophoretic mobility, which we convert into an apparent zeta potential [19] with the Helmholtz-Smoluchowski equation (Eqn. 2).

Acknowledgements

This work was supported by NIH grant GM24971 and NSF grant PCM8200991.

References

1 Myers, M., Wortman, C. and Freire, E. (1984) Biochemistry 23, 1442–1448
2 Sela, B.-A. and Bach, D. (1984) Biochim. Biophys. Acta 771, 177–182
3 Goins, B., Barisas, B. and Freire, E. (1985) Biophys. J. 47, 1162
4 Brewer, G. and Thomas, P. (1984) Biochim. Biophys. Acta 776, 279–287
5 Maggio, B., Cumar, F. and Caputto, R. (1981) Biochim. Biophys. Acta 650, 69–87
6 Probst, W., Mobius, D. and Rahmann, H. (1984) Cell. Mol. Neurobiol. 4, 157–174
7 Hayashi, K. and Katagiri, A. (1974) Biochim. Biophys. Acta 337, 107–117
8 Abramson, M., Yu, R. and Zaby, V. (1972) Biochim. Biophys. Acta 280, 365–372
9 Sharom, F. and Grant, C. (1978) Biochim. Biophys. Acta 507, 280–293
10 Bertoli, E., Masserini, M., Sonnino, G., Ghidoni, R., Caestaro, B. and Tettamanti, G. (1981) Biochim. Biophys. Acta 647, 196–202
11 Behr, J. and Lehn, J. (1973) FEBS Lett. 31, 297–299
12 Muhleisen, M., Probst, W., Weigandt, H. and Rahmann, H. (1979) Life Sci. 25, 791–796
13 Probst, W., Rosner, H., Weigandt, H. and Rahmann, H. (1979) Hoppe-Seyler Z. Physiol. Chem. 360, 979–986
14 Felgner, P., Thompson, T.E., Beach, J., Barenholz, Y. and Wong, M. (1982) Biophys. J. 37, 209a
15 Jaques, L., Brown, E., Barrett, J., Brey, W. and Weltner, W. (1977) J. Biol. Chem. 252, 4533–4538
16 Czarniecki, M. and Thornton, E. (1977) Biochem. Biophys. Res. Commun. 74, 553–558
17 McLaughlin, S., Mulrine, N., Gresalfi, T., Vaio, G. and McLaughlin, A. (1981) J. Gen. Physiol. 77, 445–473
18 McLaughlin, A., Eng, W.-K., Vaio, G., Wilson, T. and McLaughlin, S. (1983) J. Membrane Biol. 76, 183–193
19 McDaniel, R., Sharp, K., Brooks, D., McLaughlin, A., Winiski, A., Cafiso, D. and McLaughlin, S. (1985) Biophys. J. in the press
20 Aveyard, R. and Haydon, D.A. (1973) Introduction to the Principles of Surface Chemistry, pp. 40–57, Cambridge University Press, Cambridge
21 McLaughlin, S., Szabo, G., Eisenman, G. and Ciani, S. (1970) Proc. Natl. Acad. Sci. USA 67, 1268–1275
22 Muhleisen, M., Probst, W., Hayashi, K. and Rahmann, H. (1983) Japan. J. Exp. Med. 53, 103–107
23 McLaughlin, S. (1977) in Current Topics in Membranes and Transport, Vol. 9, pp. 71–144, Academic Press, New York
24 Tosteson, M., Tosteson, D. and Rubnitz, J. (1980) Acta Physiol. Scand. Suppl., 21–25
25 McLaughlin, S. (1982) in Membranes and Transport (Martonosi, A., ed.), Vol. 1, pp. 51–55, Plenum Press, New York
26 McDaniel, R. and McIntosh, T. (1986) Biophys. J., in the press
27 McDaniel, R., McLaughlin, A., McLaughlin, S., Winiski, A. and Eisenberg, M. (1984) Biochemistry 23, 4618–4623
28 Sharp, K. and Brooks, D. (1985) Biophys. J. 47, 563–566
29 Levine, S., Levine, M., Sharp, K. and Brooks, D. (1983) Biophys. J. 42, 137–145